PROCEEDINGS OF SCIENCE

# Modeling the propagation and impact of CMEs on Earth's magnetosphere for enhanced space weather forecasting

**Ritesh Sharma,**[a,*] **B. Hariharan**[b] **and Venktesh Singh**[a]

[a] *Department of Physics, Central University of South Bihar, NH-120, Gaya Panchanpur Road, Gaya - 824236, Bihar, India*

[b] *Cosmic Ray Laboratory, Tata Institute of Fundamental Research Raj Bhavan, Ooty - 643001, Tamil Nadu, India*

*E-mail:* ritesh@cusb.ac.in, 89hariharan@gmail.com, venktesh@cusb.ac.in

Coronal mass ejections (CMEs) are massive eruptions of plasma from the Sun that carry magnetic fields and can disrupt Earth's magnetosphere, triggering geomagnetic storms (GMSs). Understanding their propagation and interaction with the solar wind is essential for improving the accuracy of space weather forecasts. This study employs numerical simulations to investigate the interplanetary evolution of CMEs and their interaction with Earth's magnetosphere. Using the ENLIL heliosphere model within the Community Coordinated Modeling Center(CCMC) - which utilizes a physics-based model to simulate solar wind and CMEs within the region of space influenced by the Sun - tracks the CMEs propagation from 0.1 AU to 1 AU, incorporating solar wind dynamics and Earth's magnetospheric tilt. The simulation-based study reveals key CME behaviors, including oscillatory motion, magnetic reconnection events, and significant interactions with Earth's magnetosphere, , all of which play a crucial role in the formation of GMSs. . Additionally, we analyzed the cosmic ray cutoff rigidity using the back-tracing method, which demonstrates its variability as a reliable indicator of geomagnetic modulation during CME events. These findings highlight the importance of continuous monitoring and advanced modeling for accurate space weather prediction and the protection of the technological infrastructure.

39th International Cosmic Ray Conference (ICRC2025)
15–24 July 2025
Geneva, Switzerland

ICRC 2025
The Astroparticle Physics Conference
Geneva July 15-24, 2025

*Speaker





PoS(ICRC2025)1367

## 1. Introduction

Coronal mass ejections (CMEs), which frequently originate from the Sun and spread throughout the solar system, are intense plasma and magnetic field expulsions. These events are among the most striking manifestations of solar activity, involving the ejection of about $10^{12}$–$10^{13}$ kg of plasma, along with its embedded magnetic field, into interplanetary space. The ejected material can travel across millions of kilometres, carrying a kinetic energy in the range of $10^{25}$–$10^{32}$ ergs. In particular, these eruptions may be one of the factors in the periodic reversal of the Sun's global magnetic polarity [1]. They cause enormous disruptions that have the potential to interfere with interplanetary magnetic fields as they move through the solar wind. These disruptions are the primary causes of nonrecurrent GMSs, which can have a major impact on the Earth's magnetosphere and may have an impact on power grids, satellite operations, and communication networks [2]. In the low corona — the area just above the Sun's surface where its magnetic field is very strong — observations show that CMEs often change direction, shifting in latitude and longitude rather than moving straight outward. [3–5]. The CME impact on Earth could be caused by these deflections, which were unexpected if the position of the CME source is primarily unanticipated. Alternatively, monitoring could prevent an effect from occurring if it is predicted early enough [6, 7]. The direction of the background solar magnetic gradients typically follows CME deflections [8, 9]. Globally, this translates into motion away from coronal holes and towards the heliospheric current sheet (HCS) [10, 11]. CMEs appear to be the most strongly controlling space weather effects, so it is very important to understand the path of CMEs in the corona and heliosphere as it will definitely affect the Earth directly or indirectly. Therefore, the path of CMEs and their properties will have an impact on the Earth as it passes through the corona and heliosphere. Hence, this study is very important for accurate space weather predictions.

As a CME travels across interplanetary space, it typically takes from one to several days to reach Earth, covering a distance of about 1 AU, depending on its initial speed. A crucial factor in its geoeffectiveness is the embedded interplanetary magnetic field (IMF), particularly if it has a southward orientation. This orientation allows magnetic reconnection with Earth's northward-pointing magnetospheric field lines, primarily occurring near the first Lagrange point (L1), located approximately 0.01 AU from Earth [12]. This reconnection facilitates the transfer of solar wind energy into Earth's magnetosphere, driving geomagnetic storms (GMSs) and various phenomena such as the aurorae [13]. Beyond this direct magnetic interaction, the CME compresses the magnetosphere, intensifying geomagnetic activity by enhancing the ring current and magnetospheric convection. The product of the southward magnetic field strength and its velocity is strongly correlated with the intensity of the magnetic storm, as represented by the Dst index. Moreover, CME expansion plays a critical role; greater expansion during solar cycle 24, likely due to reduced external magnetic pressure from the solar wind, may have led to weaker interplanetary CME fields, reducing their geoeffectiveness [14, 15].

Space weather effects persist due to prolonged geomagnetic disruptions following CME impacts. CMEs often reach Earth as magnetic clouds—structures characterized by smooth magnetic field rotation, strong field strength, and lower plasma temperatures—commonly modeled as magnetic flux ropes [16, 17]. These organized configurations efficiently drive extended geomagnetic storms (GMSs). Although solar wind and magnetospheric plasmas are ideally separated, magnetic



PoS(ICRC2025)1367

reconnection at L1 and the dayside magnetopause enables their interaction. This process, involving the merging of oppositely directed field lines, facilitates solar wind energy and particle entry into the magnetosphere, injecting solar energetic particles (SEPs), disturbing radiation belts, and altering ionospheric dynamics [18].

This paper is organized into the following sections, aligned with our analytical strategy. Section 2 discusses the propagation of CMEs through the heliosphere and the coordinate transformation of CME parameters, followed by Section 3, which details the numerical techniques used to simulate cosmic ray (CR) trajectories borne out of the interaction of plasma with the geomagnetic field (GMF). Finally, Section 4 summarizes the results on the propagation of CMEs, and their impacts on the Earth's environment.

## 2. Dynamics of CMEs in the Heliosphere

We investigated four major GMS events—7 May 2005, 12 July 2012, 22 June 2015, and 7 October 2015—selected from Space Weather Live archives [19], based on their strong solar flares and CME activity. Among these, the 22 June 2015 event (linked to Carrington Rotation 2165 of Solar Cycle 24 [21, 22]) was analyzed in detail due to the muon rate enhancement observed by GRAPES-3 [20]. We employed the ENLIL model [23], which solves MHD equations for important plasma properties, to model CME propagation from 0.1 to beyond 1 AU. The workflow of our modeling pipeline is illustrated in Figure 1.

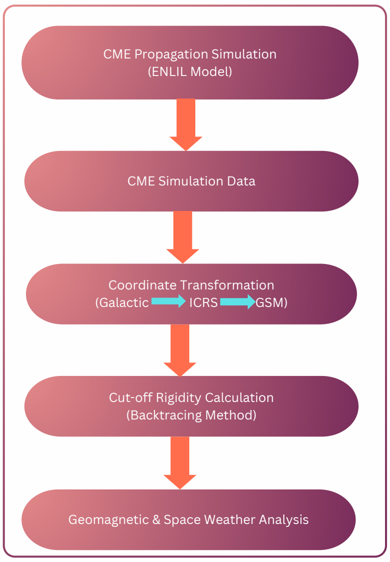


**Figure 1:** Flowchart shows the study of CME propagation in the heliosphere and their impacts in the Earth environment.

Figure 2 shows the evolution of total velocity (solid line) and magnetic field strength (dashed line) for all CME events.

ENLIL outputs are initially provided in the Heliocentric Earth Equatorial (HEEQ) coordinate system, which is a Sun-centered system used in space physics and solar physics, is suitable for heliospheric tracking but not for near-Earth interaction analysis. To estimate the CME's impact on

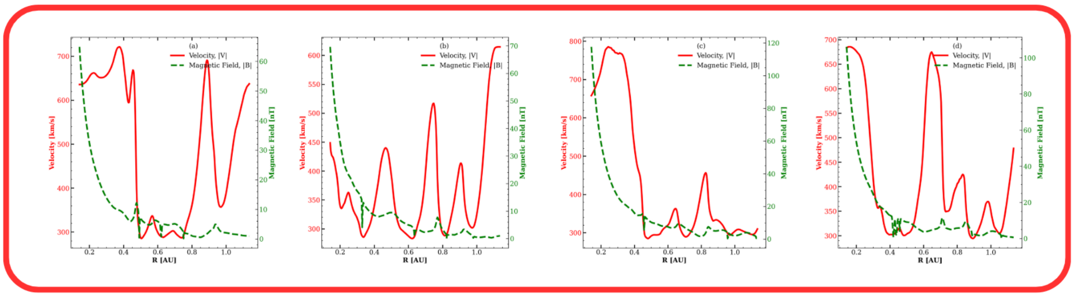

**Figure 2:** Total velocity and magnetic field variation during the propagation of all CME events.

Earth's magnetosphere, we transformed the velocity and magnetic field vectors to the Geocentric Solar Magnetospheric (GSM) frame via a two-step process. First, Galactic coordinates were rotated to the International Celestial Reference System (ICRS) using the rotation matrix provided by [28], implemented via `Astropy` [25–27]. Then, a tilt transformation with $\theta = -11^\circ$ was applied to align with Earth's magnetic dipole axis, following [29].

Figure 3 displays the GSM-transformed profiles of total velocity and magnetic field components for all CME evnets. These reveal distinct regions of CME oscillation and magnetic fields reconnection, highlighting key dynamical interactions with the ambient solar wind and IMF.

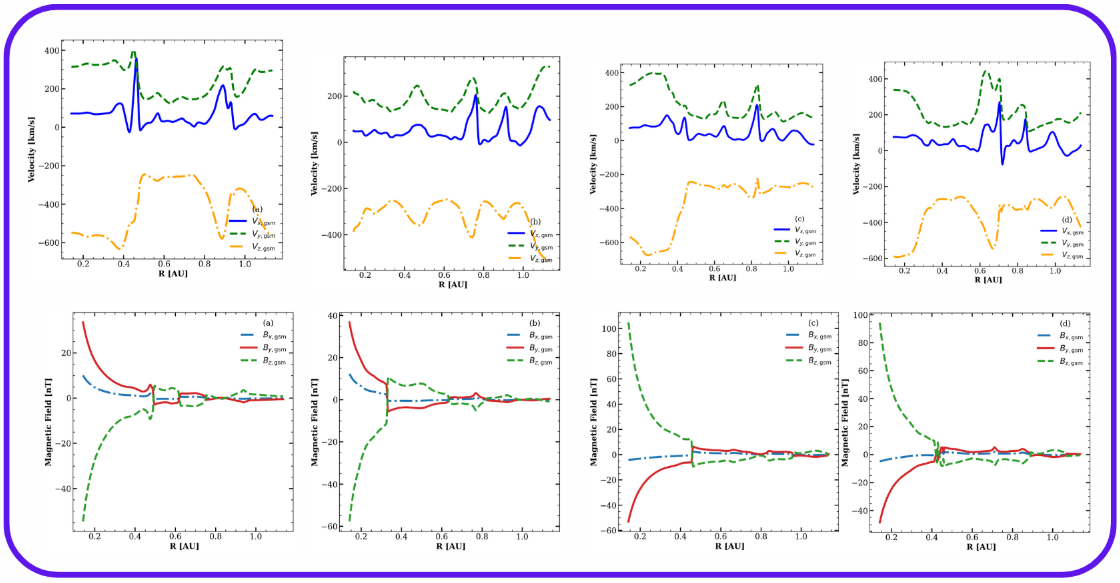

**Figure 3:** The upper panel shows the variation of velocity, while the lower panel displays the corresponding magnetic field variation in the GSM coordinate system, both plotted as a function of distance for all CME events.

## 3. Impacts on near-Earth space

Coronal mass ejections (CMEs) interacting with Earth's geomagnetic field (GMF) can induce magnetic reconnection, as well as modify the cutoff rigidity ($R$) of primary cosmic rays (CRs) and result in changes to the flux of secondary particles detected at ground level. Cutoff rigidity, defined as $R = \frac{pc}{Ze}$, represents the minimum momentum and charge ratio required for a charged particle to penetrate the GMF and reach a specific location.

We modeled the GMF using a spherical harmonic expansion of the magnetic potential $V(r, \theta, \phi)$ [29], employing Gauss coefficients and Legendre polynomials. The International Geomagnetic Reference Field (IGRF) model and the backtracing code `TJ2010` [30] were used to compute cutoff rigidity maps at GRAPES-3 (11.4°N, 76.7°E) with 1° angular resolution. Due to the high computational cost of field evaluations (~90% CPU time), we used a reference map and compared it with event-specific maps.

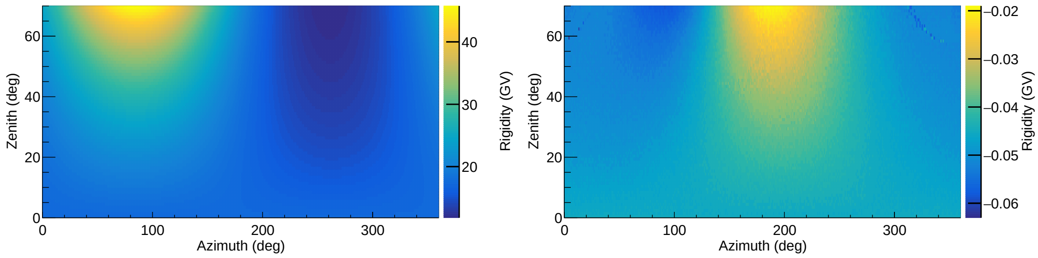


**Figure 4:** (a) Estimated cutoff rigidity map for GRAPES-3 field of view. (b) Difference in cutoff rigidity map for the 22 June 2015 event compared to the reference map.

Figure 4 shows (a) the ideal cutoff rigidity map and (b) its deviation during the 22 June 2015 GMS, revealing widespread reductions in rigidity due to magnetic reconnection. Using the CORSIKA [31] framework, we simulated 50 million primary CRs under 15 GeV–10 TeV, $\gamma$ = –2.7 conditions, and using this, we compared OmniWeb and ENLIL-driven rigidity maps with the reference spectrum and estimated the variation in the CR flux during each GMS. The results, summarized in Table 1, show that ENLIL-based estimates differ significantly, often by an order of magnitude, due to model simplifications, such as ignoring ICME magnetic structures and using empirical boundary conditions at 0.1 AU [32].

**Table 1:** List of geomagnetic storm (GMS) events with the estimated change in cosmic ray (CR) flux using the data from OmniWeb measurements and ENLIL simulation.

| GMS Event | OmniWeb (%) | ENLIL (%) |
|---|---:|---:|
| 7 May 2005 | 0.195 | −0.003 |
| 12 July 2012 | −0.039 | −0.004 |
| 22 June 2015 | 0.442 | 0.004 |
| 7 October 2015 | −0.129 | 0.008 |

Additionally, observational discrepancies arise from L1-based measurements (~1 AU), while reconnection typically occurs between 10–30 Earth radii ($R_E$). GRAPES-3 reported a muon burst during the 22 June 2015 event, which required a 40× scaling of L1 magnetic field measurements in simulations to match the observed flux [20]. This indicates missing physical information in current models during plasma transport from L1 to Earth's vicinity. Additionally, we calculated cutoff rigidities via back-tracing methods to assess cosmic ray flux changes using both OmniWeb and ENLIL data (Figure 5).



PoS(ICRC2025)1367

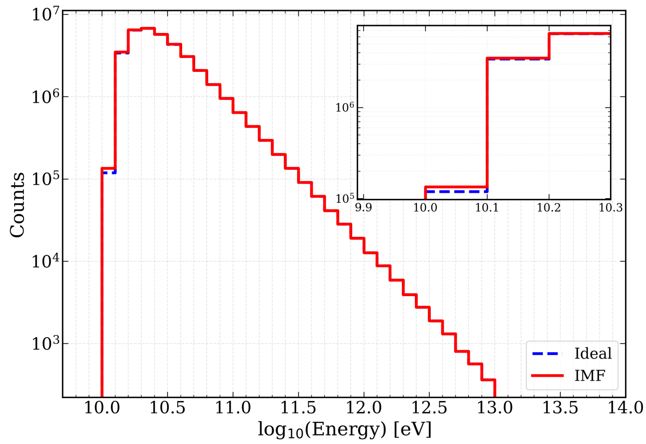


**Figure 5:** Difference in CR flux from OmniWeb for 22 June 2015 event.

## 4. Conclusions

We employed a 3D ENLIL magnetohydrodynamic model to simulate CME propagation from the Sun to Earth, capturing key dynamical behaviors and plasma–field interactions. The simulations reveal oscillatory features in the 0.13–0.26 AU range, likely due to Kelvin–Helmholtz instabilities and Alfvénic fluctuations arising from velocity shear and magnetic field modulation at the CME–solar wind interface. In the 0.40–0.53 AU region, localized magnetic reconnection events alter the CME's magnetic structure, forming plasmoids and flux ropes that contribute to plasma heating and acceleration. As the CME nears Earth (0.936–1.003 AU), it compresses the dayside magnetosphere and stretches the magnetotail, triggering geomagnetic storms with significant space weather consequences. These results highlight the critical role of CME internal dynamics and magnetospheric coupling in shaping space weather impacts.

## Acknowledgment

We acknowledge the Community Coordinated Modeling Center (CCMC) at NASA Goddard Space Flight Center for providing simulation results through their publicly available services (https://ccmc.gsfc.nasa.gov). The CORHEL-MAS_WSA_ENLIL v5.0 model was developed by Dr. Jon Linker at Predictive Science Inc., and is hosted at CCMC by Dr. Peter MacNeice, NASA Goddard Space Flight Center. The authors also thank Anne Michelle M. Mendoza, Lutz Rastaetter, Masha Kuznetsova, and Maksym Petrenko of the CCMC team for their assistance during the simulation request and execution process.

## References

[1] B. C. Low, *Coronal mass ejections, magnetic flux ropes, and solar magnetism*, *J. Geophys. Res.* **106** (2001) 25141–25163.

[2] J. T. Gosling, *The solar flare myth*, *J. Geophys. Res.* **98** (1993) 18937.

[3] E. Hildner, *CME kinematics and interplanetary phenomena*, in *Study of Travelling Interplanetary Phenomena*, vol. 71, eds. M. A. Shea, D. F. Smart, and S. T. Wu (Dordrecht: D. Reidel), 3 (1977).

[4] R. M. MacQueen, A. J. Hundhausen, C. W. Conover, *The propagation of coronal mass ejection transients*, *J. Geophys. Res.* **91** (1986) 31.

[5] A. Isavnin, A. Vourlidas, E. K. J. Kilpua, *Three-dimensional evolution of flux-rope CMEs and its relation to the solar source*, *Solar Phys.* **289** (2014) 2141, https://doi.org/10.1007/s11207-013-0468-4.

[6] M. L. Mays, B. J. Thompson, L. K. Jian, *et al.*, *Ensemble Modeling of CMEs Using the WSA–ENLIL+Cone Model*, *Astrophys. J.* **812** (2015) 145, https://doi.org/10.1088/0004-637X/812/2/145.

[7] C. Möstl, T. Rollett, R. A. Frahm, *et al.*, *Strong coronal mass ejections are not always geoeffective*, *Nat. Commun.* **6** (2015) 7135, https://doi.org/10.1038/ncomms8135.

[8] B. Gui, C. Shen, Y. Wang, *et al.*, *Quantitative Analysis of CME Deflections in the Corona*, *Solar Phys.* **271** (2011) 111–139, https://doi.org/10.1007/s11207-011-9791-9.

[9] C. Shen, Y. Wang, B. Gui, P. Ye, S. Wang, *Kinematic Evolution of a Slow CME in Corona Viewed by STEREO-B on 8 October 2007*, *Solar Phys.* **269** (2011) 389–400, https://doi.org/10.1007/s11207-011-9715-8.

[10] H. Cremades, V. Bothmer, *On the three-dimensional configuration of coronal mass ejections*, *Astron. Astrophys.* **422** (2004) 307–322, https://doi.org/10.1051/0004-6361:20035776.

[11] N. Gopalswamy, P. Mäkelä, H. Xie, S. Akiyama, S. Yashiro, *CME interactions with coronal holes and their interplanetary consequences*, *J. Geophys. Res. Space Phys.* **114** (2009) A00A22, https://doi.org/10.1029/2008JA013686.

[12] J. W. Dungey, *Interplanetary magnetic field and the auroral zones*, *Phys. Rev. Lett.* **6** (1961) 47.

[13] J. W. Chamberlain, *Theories of the Aurora*, *Adv. Geophys.* **4** (1958) 109–215, https://doi.org/10.1016/S0065-2687(08)60485-9.

[14] N. Gopalswamy, S. Akiyama, S. Yashiro, *et al.*, *Anomalous expansion of coronal mass ejections during solar cycle 24 and its space weather implications*, *Geophys. Res. Lett.* **41** (2014) 2673–2680, https://doi.org/10.1002/2014GL059858.

[15] N. Gopalswamy, S. Yashiro, H. Xie, S. Akiyama, P. Mäkelä, *Properties and geoeffectiveness of magnetic clouds during solar cycles 23 and 24*, *J. Geophys. Res. Space Phys.* **120** (2015) 9221–9245, https://doi.org/10.1002/2015JA021446.

[16] L. E. Burlaga, E. Sittler, F. Mariani, R. Schwenn, *Magnetic loop behind an interplanetary shock: Voyager, Helios, and IMP 8 observations*, *J. Geophys. Res.* **86** (1981) 6673.

[17] L. E. Burlaga, L. W. Klein, N. R. Sheeley Jr., D. J. Michels, R. A. Howard, M. J. Koomen, R. Schwenn, H. Rosenbauer, *A magnetic cloud and a coronal mass ejection*, *Geophys. Res. Lett.* **9** (1982) 1317.

[18] W. D. Gonzalez *et al.*, *Interplanetary structures responsible for intense geomagnetic storms*, *J. Geophys. Res.* **99** (1994) 5771–5792.

[19] SpaceWeatherLive Archive, *Solar activity reports and space weather data*, https://www.spaceweatherlive.com/en/archive.html, Accessed: June 2025.

[20] P. K. Mohanty *et al.*, *Transient Weakening of Earth's Magnetic Shield Probed by a Cosmic Ray Burst*, *Phys. Rev. Lett.* **117** (2016) 171101.

[21] K. Kaplan, *The Characteristic Properties of Solar Activity in Solar Cycle 24*, *Kinemat. Phys. Celest. Bodies* **40** (2024) 105–115, https://doi.org/10.3103/S0884591324020041.

[22] Astronomical League, *Carrington Rotation Start Dates*, https://www.astroleague.org/files/obsclubs/Carrington%20Rotation%20Start%20Dates.pdf, Accessed: June 2025.

[23] CCMC Model ENLIL v2.8f, https://ccmc.gsfc.nasa.gov/models/ENLIL~2.8f

[24] V. Bothmer, R. Schwenn, *The structure and origin of magnetic clouds in the solar wind*, *Ann. Geophys.* **16** (1998) 1–24, https://doi.org/10.1007/s00585-997-0001-x.

[25] Astropy Collaboration (T. P. Robitaille *et al.*), *Astropy: A community Python package for astronomy*, *Astron. Astrophys.* **558** (2013) A33.

[26] Astropy Collaboration (A. M. Price-Whelan *et al.*), *The Astropy Project: Building an Open-science Project and Status of the v2.0 Core Package*, *Astron. J.* **156** (2018) 123.

[27] Astropy Collaboration (S. L. Norman *et al.*), *The Astropy Project: Sustaining and Growing a Community-oriented Open-source Project and Status of the v5.0 Core Package*, *Astrophys. J.* **935** (2022) 167.

[28] J. C. Liu, Z. Zhu, H. Zhang, *Reconsidering the Galactic coordinate system*, *Astron. Astrophys.* **526** (2010) A16.

[29] M. A. Hapgood, *Space Physics Coordinate Transformations: A User Guide*, *Planet. Space Sci.* **40** (1992) 711–717.

[30] D. F. Smart, M. A. Shea, *A review of geomagnetic cutoff rigidities for cosmic ray studies*, *Adv. Space Res.* **36** (2005) 2012–2020.

[31] D. Heck, J. Knapp, J. N. Capdevielle, G. Schatz, T. Thouw, *CORSIKA: A Monte Carlo Code to Simulate Extensive Air Showers*, Report FZKA 6019 (1998), Forschungszentrum Karlsruhe. Available at: http://www-ik.fzk.de/corsika/physics_description/corsika_phys.html

[32] Private communications with authors of the ENLIL models.